eng

MDPI

Article

Effect of Varying Child Restraint System Seatback Angle on Spinal Loading of 1.5 YO and 3 YO PIPER Human Body Models in Frontal Impacts

Sophia K. Tushak [1], Manuel Valdano [2], Jason R. Kerrigan [1] and Francisco J. Lopez-Valdes [2,*]

[1] Center for Applied Biomechanics, Mechanical and Aerospace Engineering, University of Virginia, Charlottesville, VA 22911, USA; skt5ay@virginia.edu (S.K.T.); jrk3z@virginia.edu (J.R.K.)
[2] MOBIOS Lab, Institute for Research in Technology, Universidad Pontificia Comillas, 28015 Madrid, Spain; mvaldano@comillas.edu
* Correspondence: fjlvaldes@comillas.edu

Abstract

This computational study examined how variations in the seatback angle of two generic child restraint systems (CRSs) affect spinal loading in young occupants (1.5 YO and 3 YO) during frontal impacts, performed according to the specifications included in UNECE R129. CRS seatback angle dictates torso recline, which in turn influences head, chest, and spine kinematics and loading. While manufacturers typically recommend 30–45° for rear-facing CRSs and an upright position for forward-facing CRSs, little is known about the biomechanical implications of deviating from these guidelines. Using PIPER human body models representing a 1.5-year-old in a rear-facing CRS and a 3-year-old in a forward-facing CRS, simulations were performed under UN-R129 frontal impact conditions. The seatbacks were rotated 5° and 10° more upright or reclined relative to the nominal angle, with occupants restrained by a five-point harness and CRSs secured with ISOFIX, top tether, or three-point belt. The results showed that reclined configurations generally increased the predictions of spinal loading (forces and/or moments) given by the PIPER model, while nominal or more upright angles reduced loads, particularly in the lumbar spine of the 3-year-old model. Overall, the study highlights how computational tools can guide CRS design improvements to optimize spinal protection and enhance child safety beyond current regulatory requirements.

Keywords: child occupant; forward-facing; rear-facing; seatback angle; cervical spine; lumbar spine; PIPER

Academic Editors: Antonio Gil Bravo and Lech Bolesław Dobrzański

Received: 19 September 2025
Revised: 5 November 2025
Accepted: 22 January 2026
Published: 1 February 2026

1. Introduction

Motor vehicle crashes (MVC) remain the leading cause of children and youth aged 5 to 29 worldwide, and it is the 12th leading cause of death when all ages are considered [1]. Out of the 5,096,000 deaths in children younger than 5 years, 5.2% of these deaths can be attributed to injuries [2] resulting from different mechanisms, but with a prominent role of injuries arising from MVC. Child restraint systems (CRS) have been shown to be effective in reducing injury and death among child occupants, with studies reporting adjusted odds of injury 81.8% lower (CI: 58.3–92.1%) for toddlers in CRS compared to belted toddlers [3]. Among the countries included in the Global Status Report on Road Safety 2023, 128 reported having laws on the use of CRS, with only 37 of them meeting

WHO best practice (meaning including provisions for the minimum age and height for mandatory use of CRS, and prohibition of sitting in the front row) [1].

Among injured children hospitalized from frontal MVCs, at least one in every ten children sustained severe injury to at least one of the following regions: extremities, head, chest, abdomen, and spine [4]. Head injuries were most commonly reported for children under the age of eight, ahead of the extremities, thorax, spine, and abdomen [5]. Additionally, spinal injuries accounted for the highest proportion of moderate and severe injuries in restrained children, with injuries among young children (<4 years) attributed to flexion over the seat belt restraint (i.e., inertial loading) most often occurring in frontal impacts [6]. Further, spinal injuries have been more frequently reported in infants than toddlers [5], likely because younger children have a larger head-to-body ratio, leading to a higher location of the head–neck center of gravity.

One key aspect of CRS design affecting the likelihood of injuries is the angle of the seatback. It is of concern that other aspects such as comfort or usability can be considered a priority ahead of injury protection. For instance, most CRSs allow parents to modify the seatback angle during installation to adapt to vehicle seat geometry and the child's comfort and needs. For example, modern rear-facing infant carriers and convertible-style CRSs for rear-facing (RF) infants and forward-facing (FF) toddlers offer more granularity of seatback recline angles to enhance comfort and improve installation when switching from RF to FF, with up to 12 or more positions. Also, the question of how reclined the CRS should be has been associated with breathing airway access, especially in newborns and children up to 3 years old (YO). Literature has suggested that children aged 0 to 3 years old may need up to 16 h of uninterrupted sleep [7], preferably on a flat and firm surface [8]. As a result, current infant seats attempt to provide a position as horizontal as possible. While a recent review of the literature found that semi-upright child seats could contribute to the obstruction to the airways in neonates due to the lack of cervical muscle tone [9], this review also recommends a frequent follow up of these children so that they transition to an upright child seat as soon as it is possible and the risk for airways obstruction is minimal. This is consistent with current CRS installation recommendations [10].

Despite the above-described possibilities of choosing more recline seatback angles in current CRS, manufacturers typically recommend a seatback angle of approximately 30° to 45° with respect to the vertical for RF CRSs, while the recommended seatback angle for FF CRSs is described as an upright position [10] that is typically flush against the vehicle seat for maximum surface contact. CRS seatback angle dictates the magnitude of torso recline, which can influence the resulting kinematics and loading to the head, chest, and spine. Despite its potential influence in injury causation, current CRS designs offer the possibility of adjusting the angle of the seatback without the consideration of its effect on the biomechanical response of the child.

Although the RF configuration is recommended for infants to distribute loading uniformly over the back face of the CRS, an excessive recline angle may increase the risk of injuries. Indeed, for children in RF CRSs, surpassing the 45° limit may lead to ineffective restraint and suboptimal positioning relative to the impact vector [10]. As children grow, they transition into FF CRSs, which provide adequate level of protection for older children of the appropriate size. However, even for children that should be properly restrained for their size, a larger recline angle of the seatback may result in increased loading of the spine, particularly of the lumbar and cervical areas, as shown in reclined studies with adults [11–14].

Unfortunately, these effects of loading shifting on the spine with varying seatback angles are not easily detected in physical crash tests using pediatric anthropomorphic test devices (ATDs) or dummies. There is unquestionable evidence of the lack of biofidelity of

pediatric ATDs when it comes to assess spinal loading, due to the lack of the appropriate spinal compliance resembling the human spine [15–21]. In this scenario, computational human body models (HBM) provide the opportunity of assessing the influence of CRS seatback change on the loads of the spine.

Thus, the goal of this study is to elucidate the effects of varying CRS seatback angle on spinal loading in frontal impacts performed according to the specifications of UNECE R129, with a focus on cervical and lumbar regions, using a computational HBM of a pediatric occupant.

2. Materials and Methods

2.1. Occupant Models

The PIPER Scalable Child HBM was released at the end of the PIPER project and was made available online under a free licensing scheme (EU FP7/2007-2013, grant agreement 605544). The model was based on previous efforts carried out within the CASPER EU funded project (2008–2012) and showed potential for the study of the kinematics and interaction with CRSs.

The original child PIPER model targeted the age range between 1.5 YO and 6 YO with potential to be extended to 10 YO. The internal and external geometry of the model was derived from CT scans obtained from children in combination with the statistical shape model developed by UMTRI (http://childshape.org). Detailed information about the development of the model can be found in multiple literature references [22,23]. In the case of this study looking into the effects of seatback angle change both in RF and FF seats, the 1.5 year old (1.5 YO, weight: 12.5 kg, height: 81 cm) and 3 year old (3 YO, weight: 16.0 kg, height: 93 cm) PIPER child HBMs (included in the 6 YO PIPER child model repository) were selected. These younger PIPER models were geometrically scaled versions of the stock 6 YO PIPER child model that were scaled using the PIPER tool, based on Kriging nonlinear interpolation [24]. PIPER child models were within the height and weight recommendations for their corresponding CRS, although the 1.5 YO PIPER child model was close to the upper limit of the RF infant CRS (CRS recommendation weight: 13 kg, height: 83 cm)

2.2. CRS and Test Fixture Models—Initial Conditions

The above-mentioned pediatric HBMs were paired with generic FE models of RF and FF CRSs, also included in the PIPER child model repository [21,22]. The CRS models were developed during the CASPER project. The RF CRS had a design based on the Maxi Cosi Priori Fix, modelled with an elastic seat shell (covered with a foam covering) and a rigid seat base. Validation of this model was based on comparisons with physical tests performed with the Q3 dummies. The FF CRS had a design based on the Jane Indy Racing seat. This model was validated based on sled tests with a Q6 dummy and interpolated to represent several CRSs [25]. The paired CRS and corresponding HBM were positioned on the United Nations Regulation No. 129 (UN-R129) test bench (Figure 1). At eighteen months (1.5 YO), children are suggested to be seated RF, so the generic RF CRS model was used (NHTSA, CDC, AAP, UN/ECE). Three years old is typically within the range of ages and sizes in which toddlers outgrow their RF CRS and are recommended to transition to a FF CRS in most countries (NHTSA, CDC, AAP, UN/ECE). Further, the 3 YO PIPER child model was too large for the generic RF CRS, so the generic FF CRS was selected.

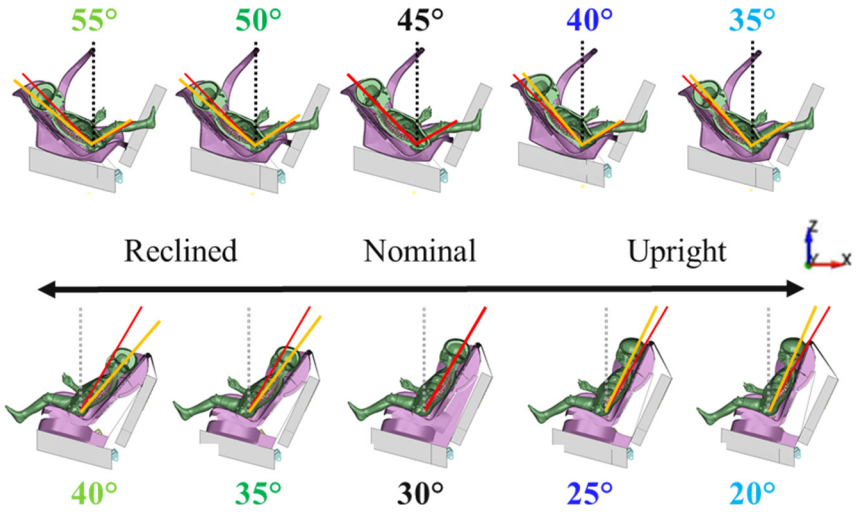

Figure 1. Mid-sagittal section of the 1.5 YO PIPER child model seated in the RF CRS (**top**) and 3 YO PIPER child model in the FF CRS (**bottom**) of varying seatback angles on the test bench. The global coordinate system is shown. Red = nominal angle and orange = modified angle, with respect to the vertical axis (dashed).

The baseline seatback angle of each CRS as it was initially defined (RF~45° and FF~30° from vertical) was considered, and then both CRSs were rotated to become more reclined or more upright (5° and 10° in each direction) to assess relative differences in the PIPER model with seatback angles within and outside manufacturer recommendations. To rotate the seatback, the elements comprising the seatback were simultaneously rotated about a node positioned at the interface between the seatback and seatpan (Figure 2). The elements at the interface region were compressed or stretched when the seatback was rotated more upright or more reclined, respectively. This process resulted in elements that were overly stretched, and the area around the rotation point was remeshed. The elements of the CRS in contact with the occupant were modelled as shells of large stiffness, simulating almost rigid elements. These elements were remeshed after the rotation to ensure numerical stability of the simulation. The elements around the rotation point were remeshed until their resulting aspect ratio was similar to the original ones, to avoid issues with contact performance or numerical instabilities.

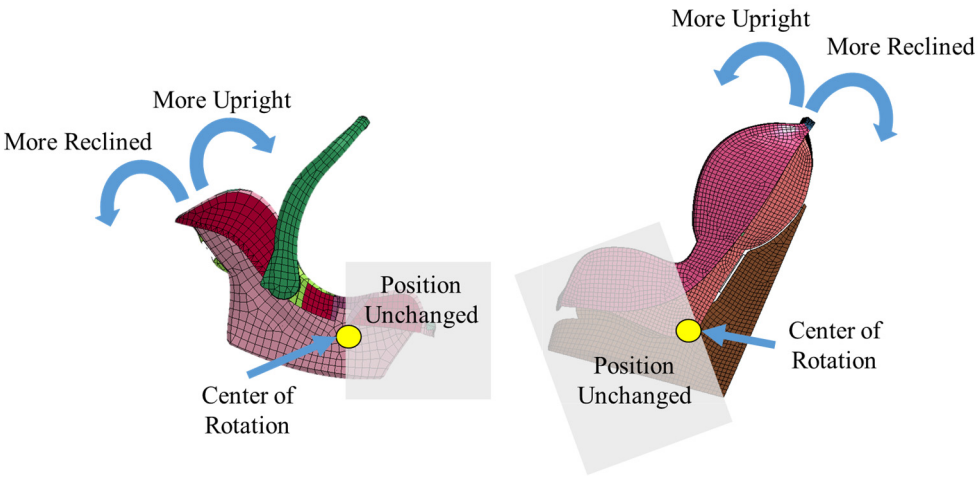

Figure 2. Visualization of seatback angle modification for the RF CRS (**left**) and FF CRS (**right**) in which the seatback was rotated about the seatpan nodes via the center of rotation, defined as the junction between the two (yellow circle).

Overall, the legs of both HBMs, which were initially bent 90 degrees at the knee, were straightened as much as possible to maintain mesh quality. All other HBMs parts were constrained to not move during leg extension. Then the HBMs were rotated as a rigid body until the back matched the seat back angle of the corresponding CRS. Last, the HBMs were settled under gravity onto the CRS using the skeleton constraints outlined in [26], so the flesh deformed but the bones did not move in the process. In the gravity settlement, the lower legs were allowed to flex at the knee. This process allowed to maintain a comparable extremity initial positioning and the same distance between the interface of the seatback/seatpan and the pelvis with all the seat back angles considered.

Five-point harness restraints of generic seat webbing material and hardware were utilized for all CRS models, and belt routing was performed in PRIMER (v18.0, Oasys Ltd., San Francisco, CA, USA). The harness consisted of shell elements with a width of 20 mm and beam elements connecting belt segments, with two belts over the shoulders and torso, two belts on the pelvic wings, and one belt between the legs (belt properties: 8 kN at 10% elongation) [27]. The RF CRS models were restrained to the test bench with a 50 mm-wide three-point belt (no pretensioners or load limiters), and the FF CRS models were restrained to the test bench with the ISOFIX mechanism (included in the PIPER repository) and two top tethers positioned side-by-side, to distribute restraint evenly across the CRS seatback and avoid yaw of the child and CRS relative to the test bench due to asymmetric restraint (belt properties: 20 kN at 10% elongation).

The friction coefficients used in the contacts between the occupants, CRS, restraint elements and test bench are listed in Table 1. The seat belt was fit via the Oasys belt fitting procedures, which removed the slack from the harness belt portions. The attachment of the three-point seat belt (RF CRS) and the top tether (FF CRS) to the test bench anchorages were modelled as 1D slipring element, using the Oasys Primer belt routing interface.

Table 1. Friction coefficients used in the modelling of restraint components.

	RF CRS	FF CRS
CRS and test bench	0.45	0.45
5-point harness and HBM	0.20	0.30
Seat belt and RF CRS	0.30	--
Seat belt and anchorages in RF CRS	1D slipring	--
Top tether and FF CRS, bench	--	0.20
Top tether and anchorages in FF CRS	--	1D slipring
HBM and test bench	0.45	0.45

All models were simulated in the UN-R129 frontal crash pulse (trapezoidal with a 24 g plateau), totalling 10 simulations (LS-DYNA, R12.0.0, mpp971, ANSYS, Canonsburg, PA, USA). Lumbar spine loads at each intervertebral disc were extracted from the PIPER-defined instrumentation. Cervical spine loads were extracted from defined spinal cross-sections at the first cervical vertebra C1. SAE J211 guidelines were used to report the loads, both for the sign conventions and the filtering (cervical forces = CFC1000, cervical moments and lumbar forces and moments = CFC600).

3. Results

3.1. Rear-Facing CRS with the 1.5 YO

Figure 3 shows the kinematics of the 1.5 YO PIPER model at 0 ms, 50 ms, 100 ms and 150 ms per each of the seat-back angles analyzed. These captures show the almost equivalent initial position of the model for each of the recline angles considered. The overall kinematics of the 1.5 YO PIPER model are similar, regardless of the seat-back angle.

Figure 3. Selected video frames (0 ms, 50 ms, 100 ms, 150 ms) in columns showing the kinematics of the 1.5 YO PIPER HBM for the different seat-back angles (in rows).

Peak cervical spine shear forces and extension moments were similar regardless of seatback angle (~300 N, 5 Nm), but the reclined seatbacks displayed bi-modal behaviour compared to the unimodal behaviour of the other models (Figure 4a,c). On the other hand, peak cervical spine tension forces increased as seatback angle became more reclined (210 to 690 N) in the RF CRS configuration with the 1.5 YO model (Figure 4b).

Lumbar spine shear forces did not display a clear trend across spinal levels or seatback angles and were always less than 300 N (Figure 5). Peak lumbar spine compression forces were relatively similar across all spinal levels for each seatback angle, varying from 180 to 570 N, and were lowest in the upright positions. Tensile lumbar spine forces were larger in the two recline positions, but also remained almost constant across the whole lumbar spine (Figure 6). Peak lumbar spine flexion moment increased by descending lumbar spine level (3 to 22 Nm), and was generally lowest in the nominal CRS position (Figure 7).

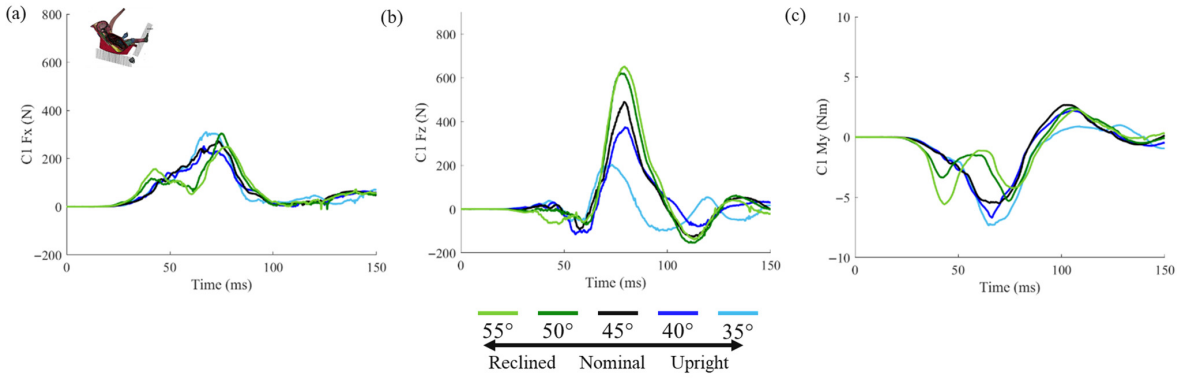

Figure 4. Cervical spine forces and moments of interest reported in the local C1 coordinate system for the 1.5 YO-RF: (**a**) Fx = anterior–posterior shear force (positive = anterior shear), (**b**) Fz = axial tension-compression force (positive = tension), and (**c**) My = flexion moment (positive = flexion).

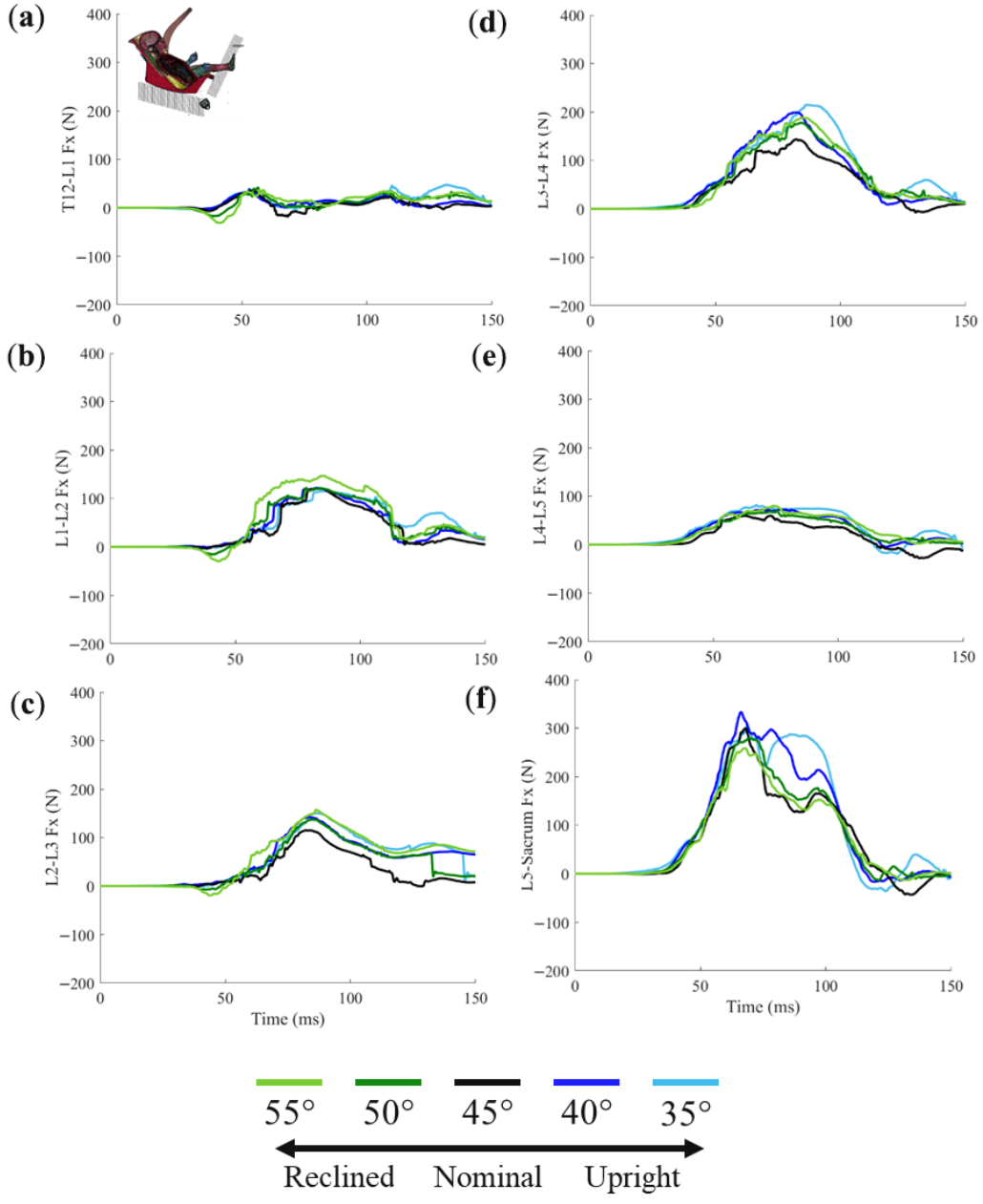

Figure 5. Lumbar spine shear force (Fx) at each intervertebral disc (**a**–**f**).

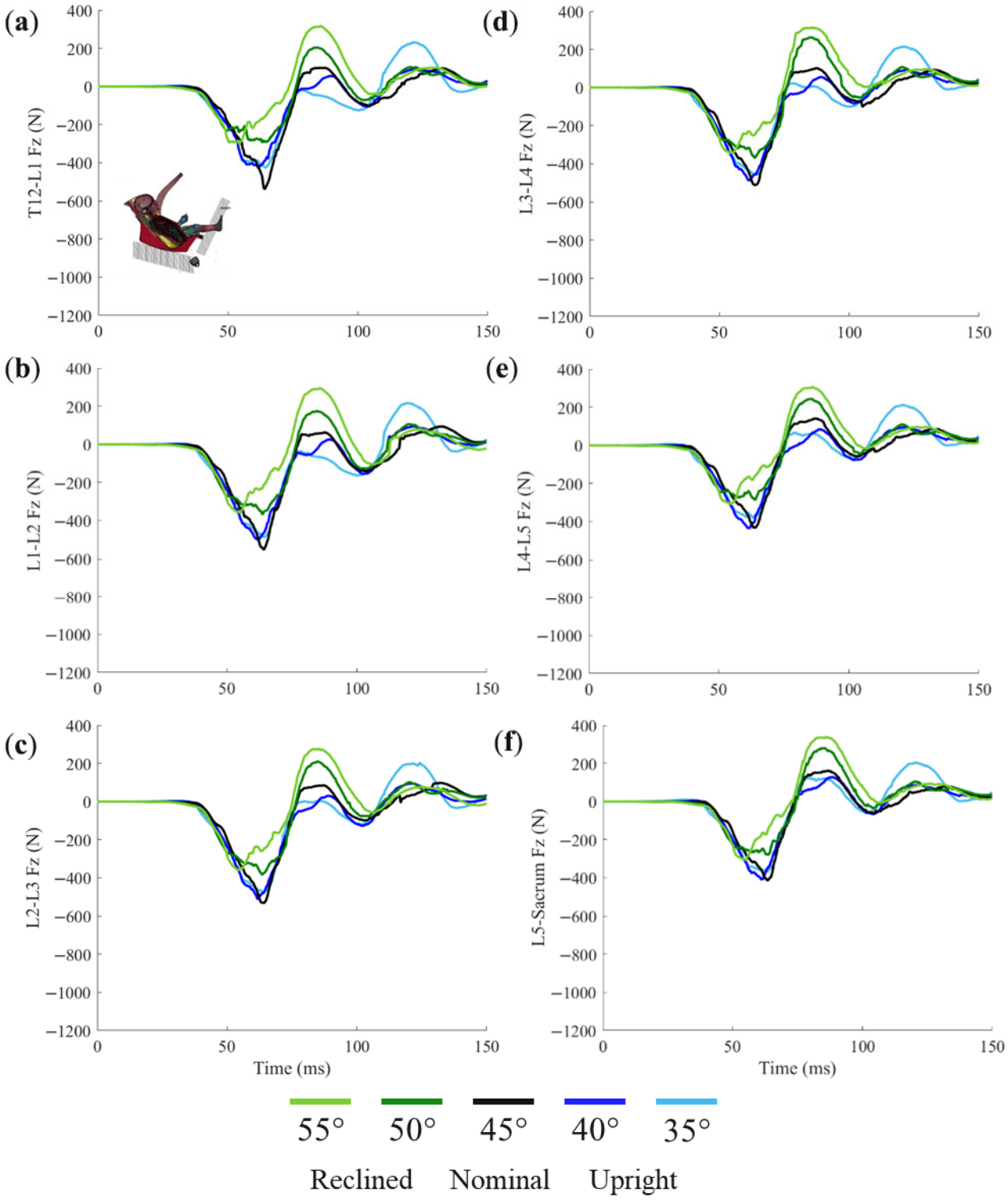

Figure 6. Lumbar spine axial force (Fz) at each intervertebral disc (**a**–**f**).

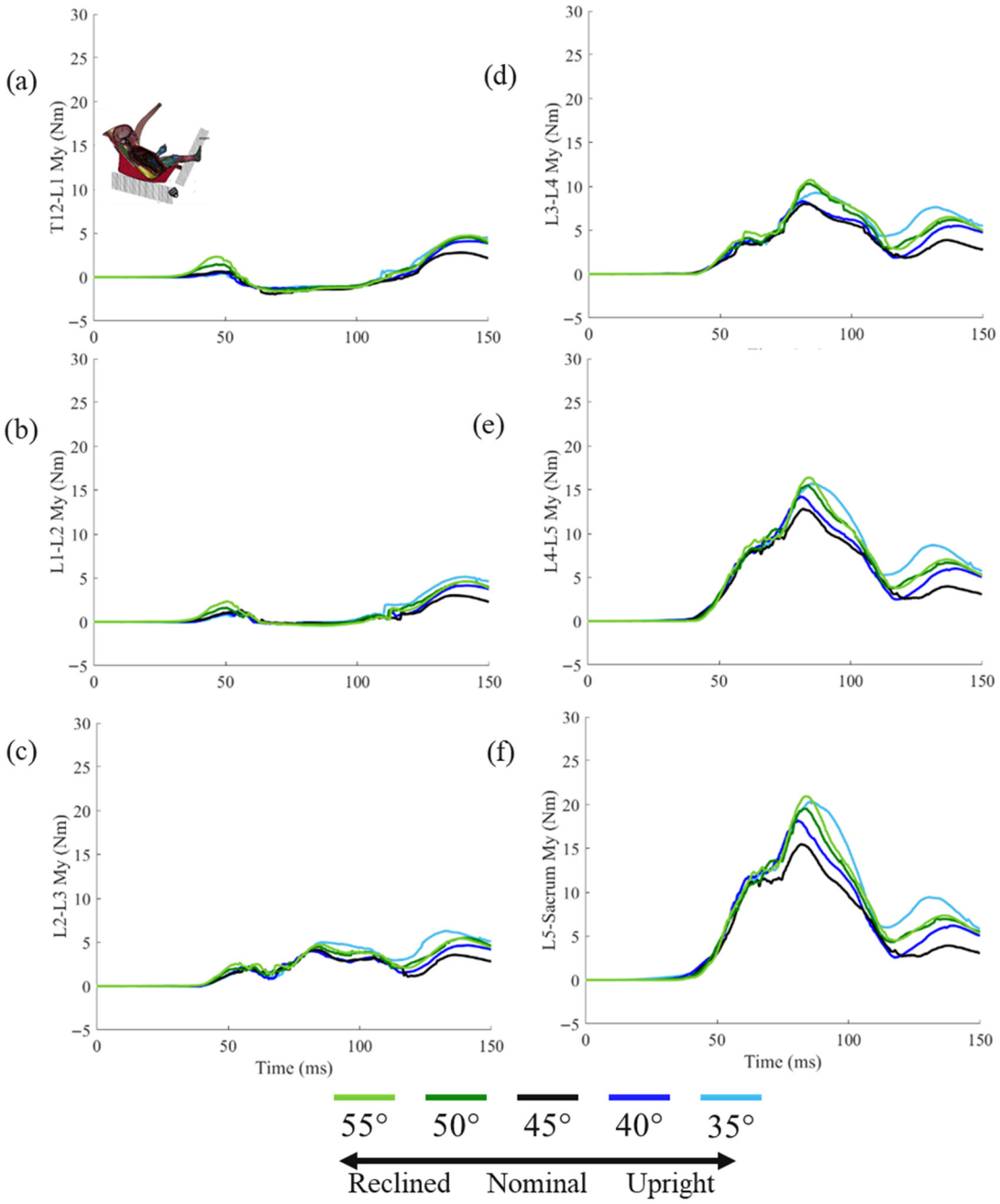

Figure 7. Lumbar spine bending moment (My) at each intervertebral disc (**a**–**f**).

3.2. Forward-Facing CRS with the 3 YO

The kinematics of the 3YO PIPER HBM in the FF CRS are included in Figure 8 for selected times during the impact and for each of the recline angles of the seat-back. The initial frames (t = 0 ms) show the similar lower extremity and pelvic positions regardless of the seat-back angle, but also illustrate the differences in the torso angle. These differences are causing the larger thoracic spine flexion observed towards the end of the impact (t = 150 ms) in the more upright positions of the seat-back, compared to the larger cervical flexion present in the more reclined positions.

Figure 8. Selected video frames (0 ms, 50 ms, 100 ms, 150 ms) in columns showing the kinematics of the 3 YO PIPER HBM for the different seat-back angles (in rows).

Peak cervical spine tension forces were similar for the nominal and upright positions (~650 N), but increased in the reclined positions (790 to 815 N). All peak cervical spine shear forces and flexion moments were of similar magnitudes (~350 N, 5 Nm) (Figure 9).

For descending spinal level, initial peak lumbar spine shear forces changed from posterior to anterior directions, ranging from about 200 to 600 N in either direction (Figure 10). Peak anterior shear forces (T12/L1-L3/L4) were consistently lower for more upright seatbacks (Figure 10), while peak posterior shear forces (L5/Sacrum) were lower for reclined seatbacks (Figure 10f). Peak lumbar spine compression forces were lowest in the most

upright position, and increased as the seatback angle became more reclined (790 to 1200 N) (Figure 11).

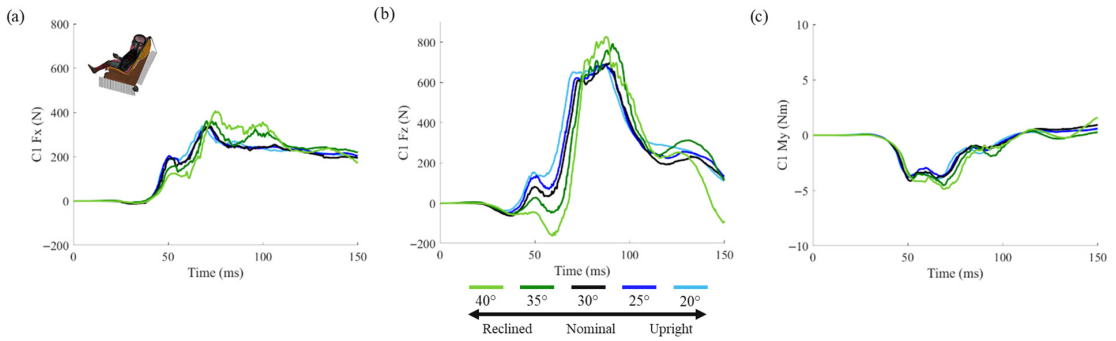

Figure 9. Cervical spine forces and moments of interest reported in the local C1 coordinate system for the 3 YO-FF: (**a**) Fx = anterior–posterior shear force (positive = anterior shear), (**b**) Fz = axial tension-compression force (positive = tension), and (**c**) My = flexion moment (positive = flexion).

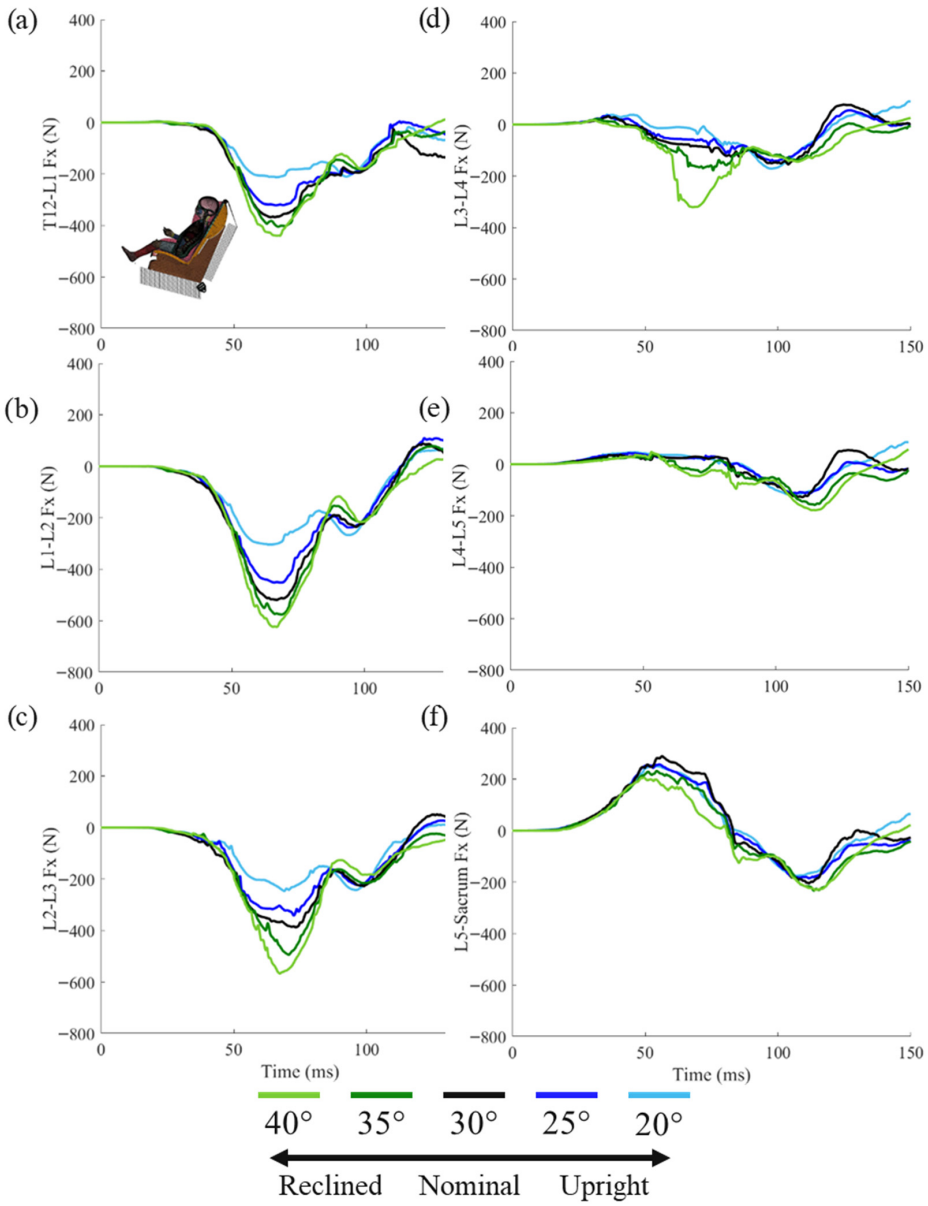

Figure 10. Lumbar spine shear force (Fx) at each intervertebral disc (**a**–**f**).

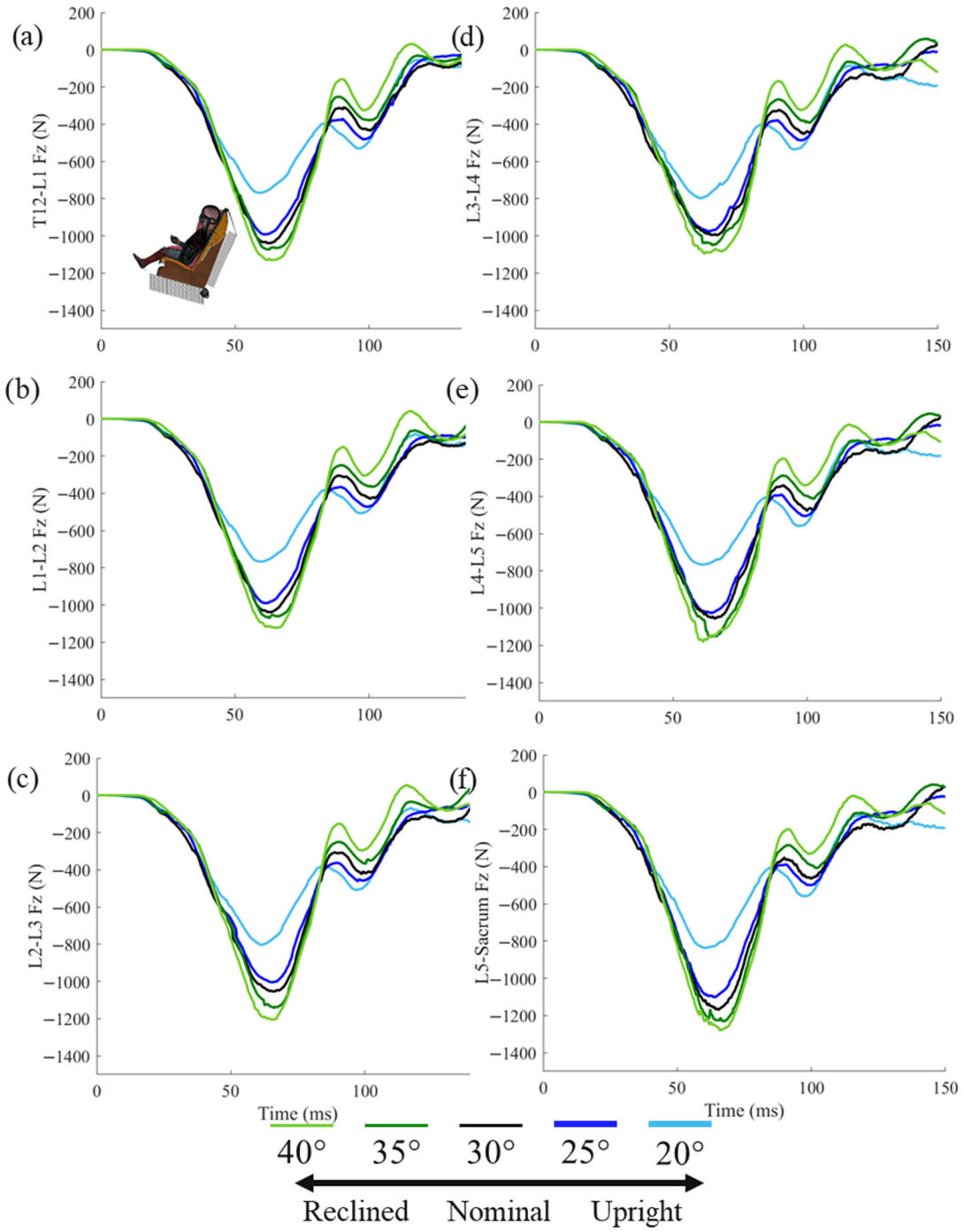

Figure 11. Lumbar spine axial force (Fz) at each intervertebral disc (**a**–**f**).

Peak lumbar spine flexion moments were lowest in the most reclined position and increased as the seatback become more upright (16 to 30 Nm) within each vertebral level (Figure 12). However, peak lumbar spine compression forces and flexion moments were of similar magnitude for each position across all six spinal levels (Figures 11 and 12).

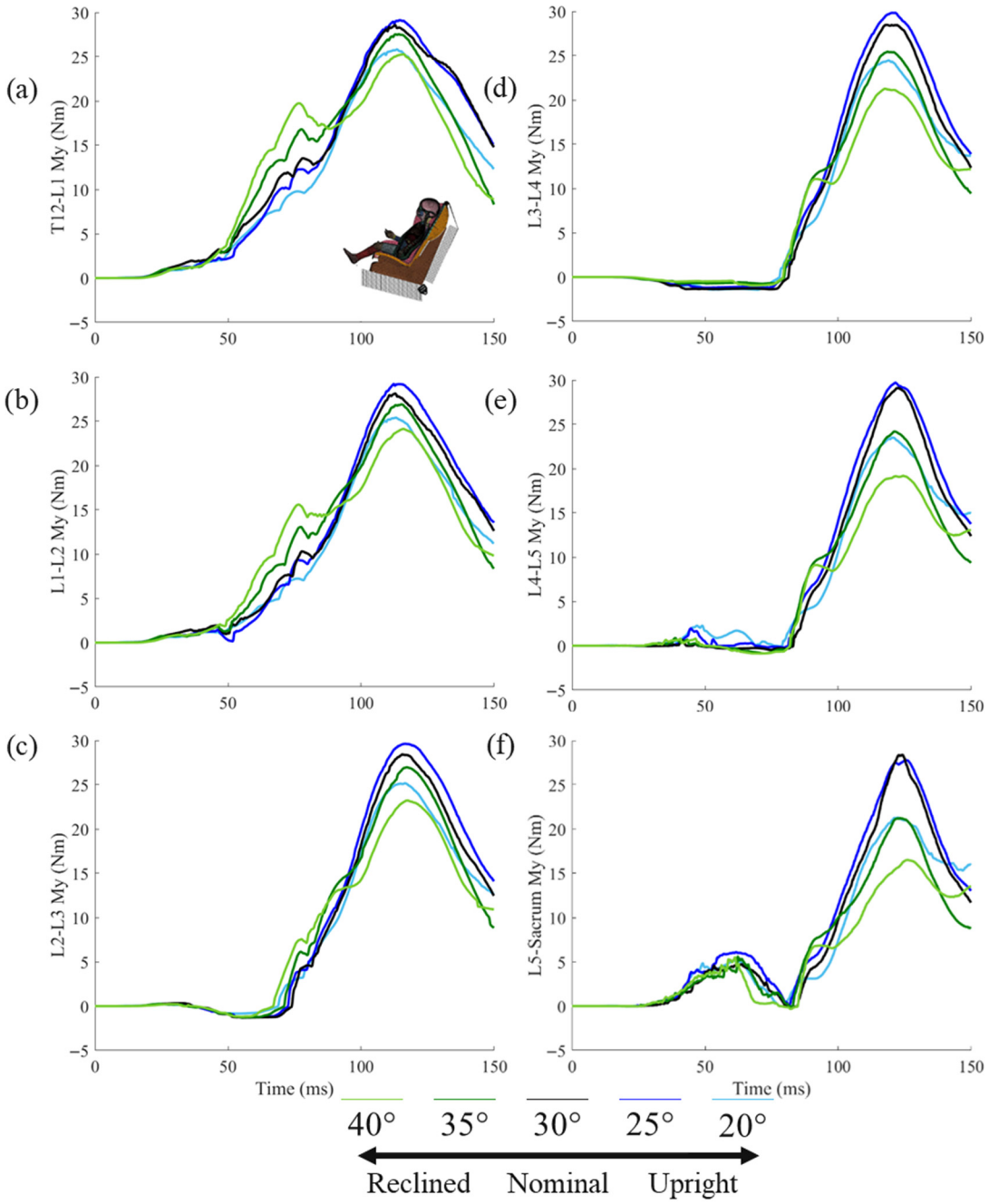

Figure 12. Lumbar spine bending moment (My) at each intervertebral disc (**a**–**f**).

4. Discussion

4.1. Rear-Facing CRS with the 1.5 YO

Despite the fact that rear-facing seats provide adequate protection to children especially in frontal impacts, this study shows that for highly reclined seats, the CRS may become too horizontal to continue to optimally protect the child. Indeed, the tensile force (Fz) increased substantially in the 35- and 40-degree recline angles compared to the nominal inclination.

As mentioned, no spinal injury criterion exists for the PIPER pediatric HBM model. Even if only for providing some perspective, it is worth comparing the peak values obtained in the simulations with available experimental data obtained from tests with pediatric PMHS [28] and suggested injury metrics of pediatric dummies [29]. The tensile forces obtained in this study regardless of the seatback angle are within the failure tensile forces measured by Ouyang et al. (range 494 to 918 N) in a sample including 12 pediatric donors

aged 2 to 12 years, and show that failure tolerance increased with age. Following this trend, the tensile tolerance for a 1.5 YO would be close to or less than approximately 500 N, although there is currently limited human data to corroborate this hypothesis. A second PMHS study tested perinatal, neonatal, and pediatric cervical spine sections in tension, including one 1.5 YO donor that failed between approximately 700 to 900 N, depending on the spinal section. They also observed an increase in failure tolerance with child age, with a significant, nonlinear relationship between the two variables, with reasonable 1.5 YO cervical spine section failure to begin between 500 and 850 N [30]. Ultimately, the cervical spine loads predicted by the reclined 1.5 YO PIPER child model indicated potentially injurious loading conditions in the current study, although the PIPER child model spine biofidelity remains questionable. If the PIPER pediatric HBM is compared to the corresponding Q1.5 ATD, the results shown here are far from reaching the tolerance values proposed in [29] (tension force = 2000 N, flexion moment = 30 Nm), although it is known that pediatric dummies exhibit a stiffer neck response.

In comparison to a 1.5 YO ATD multi-body model (Q1.5) in similar loading conditions [31], the peak cervical spine axial forces and shear forces in the nominal case were substantially lower and higher, respectively, than those for the PIPER child model. However, peak resultant sagittal forces (axial + shear) were similar between the two studies (~550 N). Relative to the nominal seatback angle, cervical spine axial forces displayed different behaviours, in which the PIPER cervical spine always reported tensile forces, while the ATD multi-body model cervical spine reported tensile forces for reclined seatbacks and compressive forces for the upright seatbacks. Variation in findings, in conjunction with fundamental differences among these human surrogates (ATD vs. human, and multibody vs. FE), suggest the potential need for surrogate-specific injury metrics for injury risk assessment and better understanding of what is causing these differences. Unfortunately, we do not have a set of physical tests with the Q1.5 dummy to compare to.

Increasing the recline angle resulted in an increase in the tensile force in the lumbar spine, and any deviation from the nominal seatback position contributed to an increase the flexion moment, especially in the lower sections of the lumbar spine.

Ultimately, the results from this study indicate that the current RF CRS seatback angle design recommendations (30 to 45°) are optimal for the most spinal loading, and any additional recline past the current range (>45°) may introduce adverse effects on these measurements.

4.2. Forward-Facing CRS with the 3 YO

All 3 YO child models experienced chin-to-chest contact at approximately the same time in the simulation (79.8 ± 1.3 ms). Chin-to-chest contact has been previously described with the use of age-matched ATDs (Q3) and FF CRSs in the UN-R129 frontal impact condition, which generally occurred later in the impact and resulted in higher peak cervical spine tension than if contact did not occur [32].

As with the RF 1.5 YO case, the measured axial loads were within the range of failure tension forces for pediatric cervical spines (range: 494 to 918 N, 2–12 YO subjects [28]), and close to the failure tension forces in which the 3 YO donors failed (570 and 817 N). Similarly, Luck et al.'s statistical model that related cervical failure tensile force based on child age would predict a 3 YO cervical spine section to begin to fail at around 700 N [30], indicating possibly injurious scenarios for all seatback angles. Field data show that the head and spine sustain the highest proportion of injuries and fatalities for young children in FF CRSs in frontal MVCs [15,33]. Head injuries without any evidence of head contact with the car interior have been associated with neck tension corresponding to upper neck injuries when impact speeds were relatively high [15,34], providing relevance to the simulation

conditions in this study in which neck loading was inertial. This in-depth case review has indicated that the serious and fatal non-contact head injuries and cervical spine injuries occurred in younger children (one to four years old) that were well-restrained, likely due to the incomplete ossification and relatively high flexibility of the young cervical spine.

Additionally, reclined forward-facing adult occupants have been shown to experience higher magnitudes of compression forces and flexion moments in the lumbar spine [11–14], and this held true for the 3 YO in a FF CRS in the UN-R129 frontal impact. In the highest reclined seatback case, peak lumbar spine loads reached over 1200 N (compression) and 25 Nm (flexion), which are close to the lower end of the reported failure tolerance of the adult lumbar spine in high-rate dynamic compression and flexion loading [35].

Ultimately, the results from this study indicate that the current and more upright FF CRS seatback angles (20–30°) are more optimal for most modes of spine loading compared to reclined seatback angles.

4.3. Limitations

The PIPER child model is one of the most advanced child HBMs but is still a relatively new tool. Other existing child HBMs were created by scaling down adult geometry, which does not account for anthropomorphic and anatomic differences between children and adults. The PIPER child model was developed primarily from child data [22], which is generally scarce in injury biomechanics. Further, the lack of comparable biological data causes large gaps in knowledge of pediatric injury risk, as well as inaccuracies when developing other methods for assessing injury risk, such as HBMs and ATDs. Data on pediatric injury associated with trauma and MVCs (e.g., biological injury data and field data) remains scarce and continues to pose a challenge when developing child surrogates. In particular, the values of the forces and moments obtained from the simulations performed here with the PIPER model could not be compared to experimental values, as there are no experimentally based spinal injury criteria that can be applied to the PIPER model to estimate injury risk.

While the limitations in the validation of the pediatric PIPER HBM need to be recognized, it is no less important to point out that the model was based on the actual anthropometry of children and that, whenever possible, the mechanical properties of pediatric tissue have been used. When these properties were not available, adult tissue mechanical properties were used. Despite this limitation, and considering that the alternative is only the use of pediatric dummies that are well known to be substantially less compliant than human beings, especially when focusing on the spine [15–17], we believe that the trends discussed in this study are relevant to understand the potential risks associated with changing the recline angle of the seatback of CRSs. To our knowledge, this is the first time that the pediatric PIPER HBM is used to analyze how forces and moments change in the cervical and lumbar spine when the angle of the seatback changes. This study is particularly relevant as it is not rare to find CRSs with adjustable seatback positions in the market.

The generic CRS models used in this study were selected because they were open-source, included with the PIPER child model, and allow the opportunity for this study to be reproduced and expanded upon. Their use within the literature has not been frequent. It should be noted that while assessing absolute measurements of kinematics and spinal loads is valuable, this study was aimed towards evaluating relative differences between seatback angles. Similarly, the performance, in terms of validation, of the CRS models after modifying the seatback angle was not assessed, and was therefore assumed to not be significantly different from the stock, nominal CRS model. Secondarily, the RF CRS was rotated such that the angle of the bottom edge changed, which could have affected the

interaction of the modified CRSs with the test bench. This did not occur when rotating the FF CRS; the CRS structure interfacing with the test bench maintained its geometry. It should be noted that none of these modifications could be tested physically, as the CRS model is a generic one capable of providing a reasonable approximation of a CRS of its characteristics, but without resembling a specific restraint system. Positioning the PIPER child model in the RF CRS and test bench such that the legs were in front of the test bench seatback was not possible due to the allowable distance and achievable leg rotation. Thus, the child model was positioned with straighter legs that initially penetrated the test bench seatback. Lastly, for the RF CRS, the ISOFIX mechanism was not utilized, since that finite element CRS model did not include the capability.

It should also be noted that the results included in this study corresponded only to the crash test conditions and the test bench used in the frontal configuration described in regulation UNECE R129. Other crash pulses, crash directions, different vehicle seat stiffness and geometry, different seat belt properties, etc., while extremely relevant, are beyond the scope of this study.

4.4. Summary

This study made use of the pediatric PIPER HBM and generic models of CRSs to provide insight about how cervical and lumbar spinal loads shift with various angles of seatback recline. Despite the limitations in the biofidelity and validation results of the models used, this manuscript suggests that the current recommendations of CRS installation constitute an optimal solution to keep both cervical and lumbar loads within biomechanically reasonable values. In particular, current RF CRS seatback angle design recommendations (30 to 45°) are optimal for the most spinal loading, and any additional recline past the current range (>45°) may introduce adverse effects to these measurements. Secondly, more upright FF CRS seatback angles (20–30°) are more optimal for most modes of spine loading compared to reclined seatback angles.

Author Contributions: Conceptualization, S.K.T., J.R.K. and F.J.L.-V.; methodology, S.K.T., F.J.L.-V. and M.V.; formal analysis, S.K.T.; investigation, S.K.T. and M.V.; resources, J.R.K. and F.J.L.-V.; data curation, S.K.T.; writing—original draft preparation, S.K.T. and F.J.L.-V.; writing—review and editing, S.K.T., M.V., J.R.K. and F.J.L.-V.; supervision, F.J.L.-V.; project administration, J.R.K. and F.J.L.-V.; and funding acquisition, J.R.K. and F.J.L.-V. All authors have read and agreed to the published version of the manuscript.

Funding: This research was supported by the Institute for International Education (IIE) Graduate International Research Experience (GIRE) fellowship program under National Science Foundation (NSF) Grant No. 1829436. The authors report there are no competing interests to declare.

Institutional Review Board Statement: Not applicable.

Informed Consent Statement: Not applicable.

Data Availability Statement: The original contributions presented in the study are included in the article, further inquiries can be directed to the corresponding author.

Conflicts of Interest: The authors declare no conflicts of interest.

Abbreviations

The following abbreviations are used in this manuscript:

CRS	Child Restraint System
MVC	Motor Vehicle Crashes
WHO	World Health Organization
RF	Rear Facing

FF	Forward Facing
HBM	Human Body Model
EU	European Union
CT	Computed Tomography
YO	Years Old
NHTSA	National Highway Traffic Safety Administration
CDC	Centers for Disease and Control
AAP	American Academy of Pediatrics
UN-ECE	United Nations Economic Commission for Europe
PMHS	Post-Mortem Human Subject
ATD	Anthropomorphic Test Device

References

1. *Global Status Report on Road Safety 2023*, 1st ed.; World Health Organization: Geneva, Switzerland, 2023.
2. Villavicencio, F.; Perin, J.; Eilerts-Spinelli, H.; Yeung, D.; Prieto-Merino, D.; Hug, L.; Sharrow, D.; You, D.; Strong, K.L.; Black, R.E.; et al. Global, regional, and national causes of death in children and adolescents younger than 20 years: An open data portal with estimates for 2000–21. *Lancet Glob. Health* **2024**, *12*, e16–e17. [CrossRef]
3. Zaloshnja, E.; Miller, T.R.; Hendrie, D. Effectiveness of Child Safety Seats vs Safety Belts for Children Aged 2 to 3 Years. *Arch. Pediatr. Adolesc. Med.* **2007**, *161*, 65. [CrossRef]
4. Brown, J.K.; Jing, Y.; Wang, S.; Ehrlich, P.F. Patterns of severe injury in pediatric car crash victims: Crash Injury Research Engineering Network database. *J. Pediatr. Surg.* **2006**, *41*, 362–367. [CrossRef]
5. Hanna, R. *Children Injured in Motor Vehicle Crashes*; National Highway Traffic Safety Administration: Washington, DC, USA, 2010.
6. Zonfrillo, M.R.; Locey, C.M.; Scarfone, S.R.; Arbogast, K.B. Motor Vehicle Crash–Related Injury Causation Scenarios for Spinal Injuries in Restrained Children and Adolescents. *Traffic Inj. Prev.* **2014**, *15*, S49–S55. [CrossRef]
7. Stanford Children's Health. *Infant Sleep*; Stanford Children's Health: Palo Alto, CA, USA, 2025.
8. Moon, R.Y. Task Force on Sudden Infant Death Syndrome. SIDS and other sleep-related infant deaths: Updated 2016 recommendations for a safe infant sleeping environment. *Pediatrics* **2016**, *138*, e20162938. [CrossRef]
9. Davis, N.L.; Shah, N. Use of car beds for infant travel: A review of the literature. *J. Perinatol.* **2018**, *38*, 1287–1294. [CrossRef] [PubMed]
10. Nahum, A.M.; Melvin, J.W.; Yoganandan, N. (Eds.) *Accidental Injury: Biomechanics and Prevention*, 3rd ed.; Springer: New York, NY, USA, 2015.
11. Gepner, B.; Draper, D.; Mroz, K.; Richardson, R.; Ostling, M.; Pipkorn, B.; Forman, J.; Kerrigan, J. Comparison of Human Body Models in Frontal Crashes with Reclined. In Proceedings of the International Research Conference on the Biomechanics of Impact, IRCOBI, Florence, Italy, 11–13 September 2019.
12. Rawska, K.; Gepner, B.; Moreau, D.; Kerrigan, J. Submarining sensitivity across varied seat configurations in autonomous driving system environment. *Traffic Inj. Prev.* **2020**, *21*, S1–S6. [CrossRef] [PubMed]
13. Richardson, R.; Jayathirtha, M.; Chastain, K.; Donlon, J.-P.; Forman, J.; Gepner, B.; Östling, M.; Mroz, K.; Shaw, G.; Pipkorn, B.; et al. Thoracolumbar spine kinematics and injuries in frontal impacts with reclined occupants. *Traffic Inj. Prev.* **2020**, *21*, S66–S71. [CrossRef] [PubMed]
14. Shin, J.; Donlon, J.P.; Richardson, R.; Espelien, C.; Sochor, S.; Gallaher, M.; Luong, V.; Gepner, B.; Forman, J.; Östling, M.; et al. Comparison of thoracolumbar spine kinematics and injuries in reclined frontal impact sled tests between mid-size adult female and male PMHS. *Accid. Anal. Prev.* **2023**, *193*, 107334. [CrossRef]
15. Sherwood, C.P.; Shaw, C.G.; Van Rooij, L.; Kent, R.W.; Crandall, J.R.; Orzechowski, K.M.; Eichelberger, M.R.; Kallieris, D. Prediction of Cervical Spine Injury Risk for the 6-Year-Old Child in Frontal Crashes. *Traffic Inj. Prev.* **2003**, *4*, 206–213. [CrossRef]
16. Ash, J.; Sherwood, S.; Abdelilah, Y.; Crandall, J.; Parent, D.; Kallieris, D. Comparison of anthropomorphic test dummies with a pediatric cadaver restrained by a three-point belt in frontal sled tests. In Proceedings of the 21st International Technical Conference on the Enhanced Safety of Vehicles (ESV) Conference, Stuttgart, Germany, 15–18 June 2009.
17. Lopez-Valdes, F.J.; Forman, J.; Kent, R.; Bostrom, O.; Segui-Gomez, M. A comparison between a child-size PMHS and the Hybrid III 6 YO in a sled frontal impact. *Ann. Adv. Automot. Med.* **2009**, *53*, 237–246.
18. Lopez-Valdes, F.J.; Lau, S.; Riley, P.; Lamp, J.; Kent, R. The biomechanics of the pediatric and adult human thoracic spine. *Ann. Adv. Automot. Med.* **2011**, *55*, 193–206.
19. Lopez-Valdes, F.J.; Seacrist, T.; Arbogast, K.B.; Balasubramanian, S.; Maltese, M.R.; Tanji, H.; Higuchi, K.; Kent, R. A Methodology to Estimate the Kinematics of Pediatric Occupants in Frontal Impacts. *Traffic Inj. Prev.* **2012**, *13*, 393–401. [CrossRef]

20. Seacrist, T.; Balasubramanian, S.; Garcia-Espana, J.F.; Maltese, M.R.; Arbogast, K.B.; Lopez-Valdes, F.J.; Kent, R.W.; Tanji, H.; Higuchi, K. Kinematic Comparison of Pediatric Human Volunteers and the Hybrid III 6-Year-Old Anthropomorphic Test Device. *Ann. Adv. Automot. Med.* **2010**, *54*, 97–108. [PubMed]
21. Seacrist, T.; Arbogast, K.B.; Maltese, M.R.; Garcia-Espana, J.F.; Lopez-Valdes, F.J.; Kent, R.W.; Tanji, H.; Higuchi, K.; Balasubramanian, S. Kinetics of the cervical spine in pediatric and adult volunteers during low speed frontal impacts. *J. Biomech.* **2012**, *45*, 99–106. [CrossRef] [PubMed]
22. Beillas, P.; Giordano, C.; Alvarez, V.; Li, X.; Ying, X.; Chevalier, M.-C.; Kirscht, S.; Kleiven, S. Development and performance of the PIPER scalable child human body models. In Proceedings of the 14th International Conference on the Protection of Children in Cars, Munich, Germany, 8–9 December 2016; p. 19.
23. Beillas, P.; Wang, X.; Lafon, Y.; Frechede, B.; Janak, T.; Dupeux, T.; Mear, M.; Pacquaut, G.; Chevalier, M.-C.; Le Ruyet, A. *PIPER EU Project Final Publishable Summary*; IFSTTAR-Institut Français des Sciences et Technologies des Transports, de l'Aménagement et des Réseaux: Marne-la-Vallée, France, 2017.
24. Jolivet, E.; Lafon, Y.; Petit, P.; Beillas, P. Comparison of Kriging and Moving Least Square Methods to Change the Geometry of Human Body Models. *Stapp Car Crash J.* **2015**, *59*, 337–357. [CrossRef] [PubMed]
25. Giordano, C.; Li, X.; Kleiven, S. Performances of the PIPER scalable child human body model in accident reconstruction. *PLoS ONE* **2017**, *12*, e0187916. [CrossRef]
26. Miller, M.; Perez-Rapela, D.; Gepner, B.; Edwards, M.; Jermakian, J.; Forman, J. A methodology for large-scale parametric evaluation of child booster seats. In Proceedings of the IRCOBI Conference, Online, 1–2 June 2021; pp. 593–615.
27. Zhang, X.; Gao, J.; Tu, W. Parameter Study for Child Booster Seats in Frontal Collisions. *Appl. Sci.* **2023**, *13*, 2206. [CrossRef]
28. Ouyang, J.; Zhu, Q.; Zhao, W.; Xu, Y.; Chen, W.; Zhong, S. Biomechanical assessment of the pediatric cervical spine under bending and tensile loading. *Spine* **2005**, *30*, 716. [CrossRef]
29. *CLEPA Proposal for the 04 Series of Amendments to UN Regulation No. 129 (Enhanced Child Restraint Systems)*; CLEPA: Geneva, Switzerland, 2020.
30. Luck, J.F.; Nightingale, R.W.; Loyd, A.M.; Prange, M.T.; Dibb, A.T.; Song, Y.; Fronheiser, L.; Myers, B.S. Tensile mechanical properties of the perinatal and pediatric PMHS osteoligamentous cervical spine. *Stapp Car Crash J.* **2008**, *52*, 107–134.
31. Valdano, M.; Asensio-Gil, J.M.; Jiménez-Octavio, J.R.; Cabello-Reyes, M.; Vasserot-Tolmos, R.; López-Valdés, F.J. Parametric Analysis of the Effect of CRS Seatback Angle in Dummy Measurements in Frontal Impacts. In Proceedings of the IRCOBI Conference, Porto, Portugal, 14–16 September 2022.
32. Visvikis, C.; Thurn, C.; Kettner, M.; Müller, T. The effect of chin-to-chest contact on upper neck axial force in UN Regulation No. 129 frontal impact tests of child restraint systems. *Traffic Inj. Prev.* **2020**, *21*, S173–S176. [CrossRef] [PubMed]
33. Arbogast, K.B.; Cornejo, R.A.; Kallan, M.J.; Winston, F.K.; Durbin, D.R. Injuries to children in forward facing child restraints. *Annu. Proc. Assoc. Adv. Automot. Med.* **2002**, *46*, 213–230.
34. Bohman, K.; Arbogast, K.B.; Boström, O. Head Injury Causation Scenarios for Belted, Rear-Seated Children in Frontal Impacts. *Traffic Inj. Prev.* **2011**, *12*, 62–70. [CrossRef] [PubMed]
35. Tushak, S.K.; Gepner, B.D.; Forman, J.L.; Hallman, J.J.; Pipkorn, B.; Kerrigan, J.R. Human Lumbar Spine Injury Risk in Dynamic Combined Compression and Flexion Loading. *Ann. Biomed. Eng.* **2023**, *51*, 1216–1225. [CrossRef] [PubMed]